*Annual Review of Neuroscience*

# Functional Logic of a Cognitive Brain System for Navigation

Gaby Maimon[1] and L.F. Abbott[2]

[1]Laboratory of Integrative Brain Function, Howard Hughes Medical Institute, and Kavli Neural Systems Institute, The Rockefeller University, New York, NY, USA;
email: maimon@rockefeller.edu

[2]Mortimer B. Zuckerman Mind Brain Behavior Institute, Department of Neuroscience, and Kavli Institute for Brain Science, Columbia University, New York, NY, USA;
email: lfa2103@columbia.edu





## Keywords

navigation, head-direction cells, computation, *Drosophila*, vectors, coordinate transformation

## Abstract

It is unusual for cognitive neuroscientists to reach consensus around which computations a brain region implements, what algorithms are used to achieve those computations and how the algorithms are implemented by cells and circuits (i.e., Marr's three levels of analysis). Over the past decade, there has been notable progress in delineating such a unified functional understanding in the *Drosophila* central complex. In this review, we summarize how the central complex operates as a computational device that calculates the values of angles and two-dimensional vectors important for navigational behavior. Appreciating how these insights were made in *Drosophila* suggests a roadmap for reaching a similar level of understanding in larger brains.

## Contents





# INTRODUCTION

## Marr's Levels and What It Means to Understand an Information Processing System

What would it mean to say that we understand how a central brain region, such as the cerebral cortex or hippocampus, works? A definitive answer unfortunately remains unclear; however, four decades ago, David Marr (1982) laid out a well-known framework (Poggio 2012). If brain regions exist to process information, Marr argued, then a functional understanding involves separate answers to the following three questions. (*1*) What are the high-level computations being implemented by the region? (*2*) Which algorithms and representations are used to achieve these computations? (*3*) How are the algorithms physically realized in neural tissue? By identifying these separate levels, Marr's framework highlighted the importance of theory interacting with experiment to define function.

While Marr's framework is cogent, its strongest form has rarely been realized. Normative approaches have been used to identify broad computational goals and constraints, but making direct connections with biological mechanisms has proven difficult. On the experimental side, studies ranging from the biophysical dissection of single neurons and synapses to large-scale in vivo neuronal recordings have yielded insight but, typically, there is still an incomplete understanding of what the neurons, synapses and circuits are doing. Here, we describe a system where, due to a convergence of key techniques and approaches, a three-level understanding of function has been rapidly developing.

This review outlines the emerging functional logic of the insect central complex. Whereas many fundamental insights on the central complex have arisen, and continue to arise, from the study of nongenetic models (Williams 1975, Heinze & Homberg 2007, Heinze & Homberg 2008, Strausfeld 2012, Pfeiffer & Homberg 2014, el Jundi et al. 2016, Stone et al. 2017, Heinze et al. 2018, Honkanen et al. 2019, Le Moël et al. 2019, Wehner 2020, Beetz et al. 2023, Heinze 2024, Collett et al. 2025), here we focus on findings in *Drosophila*. The central complex stands out in

cognitive neuroscience because we now have a first-pass account of several core computations that this brain region performs, and these accounts extend across all three of Marr's levels. Of course, the central complex is far from solved; memory- and sleep-related functions, for example, remain a frontier. Nevertheless, the fact that structure–function relations have reached such a relatively mature state in a cognitive brain region of approximately 2,800 neurons is remarkable. This progress may help to inspire efforts to achieve a comparable state of understanding in larger brain regions within mammals.

## The Basic Components of the Insect Central Complex

The central complex is a set of interconnected neuropils found in the middle of all arthropod brains (Strausfeld 2012) (**Figure 1*a***). In insects, including *Drosophila* (**Figure 1*a***), it has four main substructures: the protocerebral bridge (or bridge), ellipsoid body, fan-shaped body, and noduli (Williams 1975; Hanesch et al. 1989; Young & Armstrong 2010a,b) (**Figure 1*b***). The protocerebral bridge is a bicycle handlebar–shaped neuropil near the back of the brain, with the fan-shaped body, ellipsoid body, and noduli positioned more anterior (**Figure 1*b***). In many dipterans (i.e., true flies), including *Drosophila*, the ellipsoid body is donut shaped, whereas in most other arthropods it is not a closed circle, resembling instead the shape of the fan-shaped body (Strausfeld 2012, Heinze 2024). Despite such variation in shape, the defining functions of the central complex structures, based on current understanding, appear to be conserved.

The central complex consists of two broad classes of neurons: columnar and tangential (Hanesch et al. 1989) (**Figure 1*c***). Columnar neurons have axonal and dendritic fields that interconnect small sectors of the bridge, fan-shaped body, and/or ellipsoid body (**Figure 1*c***, left). These subsectors are called glomeruli, tiles, wedges, or columns depending on the structure and neuron class in question (Wolff et al. 2015, Wolff & Rubin 2018). Single columnar neurons exist in discrete classes whose constituent members tessellate the bridge, fan-shaped body, and/or ellipsoid body. An EPG neuron,[1] for example, has dendrites in a single wedge in the ellipsoid body and axons[2] in one glomerulus of the protocerebral bridge (**Figure 1*c***, top left), with the full array of EPG neurons tiling these two structures. Some columnar cell classes have exactly one neuron per subsector, but most have more than one; for example, EPG cells have three to four cells per wedge in the ellipsoid body (Turner-Evans et al. 2020). Neurons in some columnar cell classes also express neurites in the noduli or other focused regions outside of the central complex, such as the gall for EPG neurons. In these neuropils, all cells of a given class converge onto a common set of input or output neurons. In *Drosophila melanogaster*, there are approximately 1,900 central complex columnar cells in around 70 different classes (Hulse et al. 2021).

Tangential cells differ from columnar cells in that the neurites of single tangential cells cut across all the subsectors of a given structure, for example, all the wedges of the ellipsoid body or all the columns of the fan-shaped body (**Figure 1*c***, right). In *D. melanogaster*, there are approximately 850 tangential cells, consisting of around 260 ring neurons in the ellipsoid body (in ∼30 classes), 570 tangential cells in the fan-shaped body (in ∼150 classes), and about 10 tangential cells in the bridge (in ∼3 classes) (Hulse et al. 2021).

[1]Central complex cells are often named after the structures they innervate. EPG neuron is thus short for ellipsoid body–protocerebral bridge–gall neuron. (EPG cells innervate the gall, a structure outside the central complex, in addition to their ellipsoid body and bridge innervations.)

[2]We refer to the parts of a neuron where synaptic input is dominant as dendrites and where synaptic output is dominant as axons. However, central complex neurons have output synapses from dendrites and input synapses to axons. We use the term neurites to refer to either dendrites or axons and for cases where input versus output is not yet functionally clear.

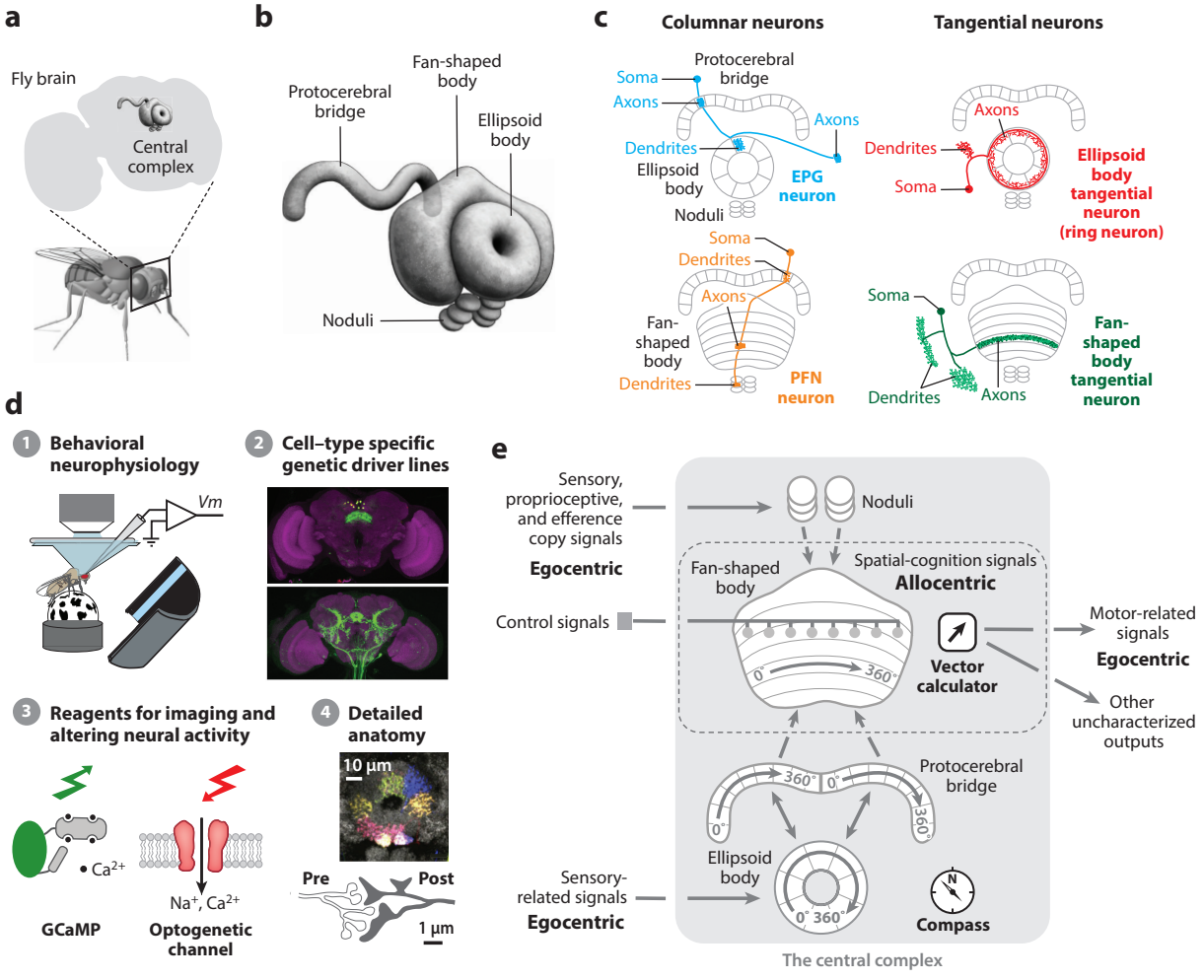


**Figure 1**

The components of the *Drosophila* central complex, its functional logic, and the methods needed to decipher this logic. (*a*) The fly brain and central complex. (*b*) Four main substructures of the central complex. (*c*) Schematized examples of two columnar neurons and two tangential neurons. (*d*) Four essential approaches that were needed to unravel a functional logic for the fly central complex. (①) Conducting patch-clamp recordings or two-photon imaging from head-fixed flying or walking flies in closed-loop virtual reality. (②) Employing thousands of GAL4, LexA, and/or Q-system driver lines to perform cell type–specific physiology. Two immunohistochemical stains of fly brains (*magenta*) in which different neuron populations express green fluorescent protein (*green*) are shown. Images were generated in the Maimon lab using GAL4 lines from Jenett et al. (2012). (③) Using genetically encoded calcium sensors and chemogenetic or optogenetic reagents to perturb neural activity. (④) Generating light- and electron microscopy–based data sets that strongly constrain or define neural circuit connectivity. The top image shows individual neurons in the ellipsoid body in different colors, using the multicolor flip-out method from Nern et al. (2015). Image adapted with permission from Green et al. (2017). The bottom schematic illustrates connectivity analyzed at the level of electron microscopy, which is now standard in the field. (*e*) This diagram summarizes a functional logic for the *Drosophila* central complex.

## WHAT WAS NEEDED TO DECIPHER THE LOGIC OF THE FLY CENTRAL COMPLEX

By the 1980s, the columnar and tangential architecture of the central complex had become clear (Hanesch et al. 1989). This layout was reminiscent of a matrix from linear algebra—with vertical

columns created by columnar cells intersecting horizontal rows created by tangential cells—suggesting that mathematical operations were taking place. However, the exact nature of these operations remained opaque for decades, until four primary experimental approaches matured (**Figure 1*d***). First, a method to measure the activity of central complex neurons during active navigational behavior was required because physiological measurements in quiescent flies were insufficient (Maimon et al. 2010, Seelig et al. 2010). Second, one needed high-quality genetic driver lines that allowed physiologists to target defined neuron classes for imaging or manipulation (Gohl et al. 2011, Jenett et al. 2012, Kvon et al. 2014, Tirian & Dickson 2017, Meissner et al. 2025, Wolff et al. 2025). Without driver lines that cleanly targeted specific cell classes, conflated signals across cell classes would have made little sense. Third, the calcium sensor GCaMP, as well as chemogenetic and optogenetic reagents, needed to mature to support both imaging and perturbing the activity of genetically defined cell populations (Zemelman et al. 2002, Lima & Miesenböck 2005, Chen et al. 2013, Klapoetke et al. 2014, Govorunova et al. 2015, Dana et al. 2016, Mohammad et al. 2017, Dana et al. 2019). Fourth, the detailed anatomy of cell classes and their synaptic interconnectivity was needed; this description was initially conducted at the light microscopy level (Lin et al. 2013, Nern et al. 2015, Wolff et al. 2015, Wolff & Rubin 2018) and then at the electron microscopy level (Zheng et al. 2018, Turner-Evans et al. 2020, Scheffer et al. 2020, Hulse et al. 2021, Schlegel et al. 2023, Dorkenwald et al. 2024, Eckstein et al. 2024). Once these methods matured, the overall logic of the system, summarized in the diagram shown in **Figure 1*e***, became explicable.

**Figure 1*e*** reveals three fundamental features of the *Drosophila* central complex. First, there is a compass in the ellipsoid body and bridge. Second, there is a vector calculator in the fan-shaped body. Third, the central complex performs computations in a map-like (e.g., north, south, east, west) or allocentric coordinate frame. Because the fly senses and moves in the world using an egocentric (e.g., front, back, right, left) reference frame, an egocentric-to-allocentric coordinate transformation is required on the input end, along with an allocentric-to-egocentric transformation on the output end, so that signals inside the central complex can interface with outside sensory and motor systems. In what follows, we describe these basic features of the central complex in depth. Although we use Marr's (1982) framing as a post hoc lens for understanding the computations of the central complex, we should note that it was not the guiding paradigm as this body of work unfolded; rather, progress was driven by the maturation of the methods described above alongside a simple curiosity regarding what this brain region might be doing, regardless of whether the eventual explanation aligned with Marr's levels or any other interpretive framework.

## FUNCTIONAL LOGIC OF THE FLY CENTRAL COMPLEX

### A Compass in the Ellipsoid Body and Bridge

EPG neurons (**Figure 1*c***) are a class of columnar cells that tile the ellipsoid body with their dendrites and the bridge with their axons (Wolff et al. 2015). At any given time, only a small subset of EPG cells are active, and coactive EPG cells always have adjacent dendrites in the ellipsoid body, which yields a localized packet of activity at one position around the donut, often called a bump of activity (Seelig & Jayaraman 2015). The ellipsoid body bump has two copies in the bridge, evident in the axon terminals of EPG cells (Green et al. 2017, Turner-Evans et al. 2017). This duplication occurs because EPG neurons project alternately to the left and right bridge as one moves around the ellipsoid body (Wolff et al. 2015), and the EPG bump spans multiple subsectors or wedges of the ellipsoid body (Seelig & Jayaraman 2015).

The EPG bump is stable when the fly is stationary, and it rotates around the ellipsoid body and correspondingly across the two sides of the bridge when the fly turns (Seelig & Jayaraman 2015,

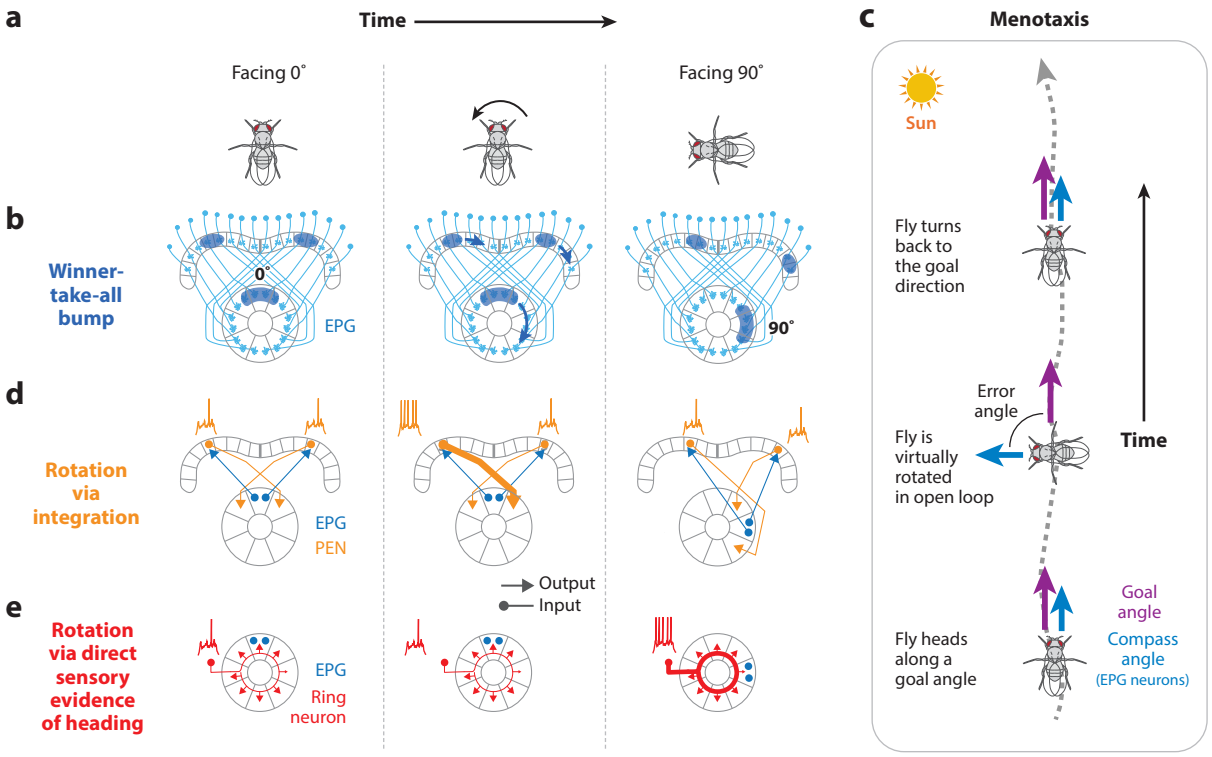


## Figure 2

The activity of EPG cells acts as a compass, tracking the fly's heading via both angular integration and direct sensory evidence. (*a*) A fly turns 90°. (*b*) The EPG bump in the ellipsoid body (in the EPG dendrites) and its two copies in the bridge (in the EPG axons) counter-rotate in the brain with respect to the fly's 90° rotation in the world. (*c*) Flies performing a task called menotaxis locomote at a consistent angle in reference to a distant cue, such as the sun, and they do so by comparing a goal angle with a heading angle. Heading and goal signals are dissociated when a fly performing menotaxis is virtually rotated in open loop. (*d*) PEN and EPG cells form a recurrent circuit that can integrate the fly's angular velocity to reposition the EPG bump when the fly turns. Specifically, EPG cells communicate their heading bump signal to PEN cells in both the left and the right bridge (*left*). When the fly turns left, PEN cells in the left bridge become more active than those in the right bridge, and due to the offset projections of PENs from the bridge to the ellipsoid body, this extra left-bridge activation induces a rotation of the EPG phase around the ellipsoid body in the correct direction (*middle*, *right*). This mechanism allows the EPG phase to update even when flies turn in complete darkness. Panel *d* adapted with permission from Green et al. (2017). (*e*) Ring neurons can reposition the EPG bump on the basis of learned associations between sensory input (such as specific visual panoramas) and bump positions around the ellipsoid body. A single ring neuron (*red*) that is activated by the visual panorama associated with the fly facing 90° is depicted. Initially the fly is facing 0°, and thus the cell is inactive (*left*). As the fly starts turning counterclockwise, the cell remains inactive (*middle*). When the fly finally faces 90°, the cell becomes activated by the now rotated visual scene (*right*). Ring neurons are generally inhibitory, and this cell has learned, due to the fly's past visual experience, to express relatively weak synaptic output on the right side of the ellipsoid body (*small red arrow*) compared to elsewhere in the ellipsoid body (*larger red arrows*). As a result, when the fly sees a visual panorama that excites this ring neuron, its activity promotes the EPG bump to reside on the right side of the ellipsoid body (i.e., the location with the weakest inhibition).

Green et al. 2017, Turner-Evans et al. 2017) (**Figure 2*a*,*b***). Each side of the bridge can be conceptualized as a structurally open, but functionally closed, circle that represents 360° of azimuthal space, akin to the 360° represented around the ellipsoid body (**Figure 1*e***). Even though the bridge appears mirror symmetric, the EPG bump copies move in parallel, like windshield wipers, around the bridge when a fly turns (i.e., in a non-mirror-symmetric fashion) (**Figure 2*b***).

The position of the bump, whether measured in the ellipsoid body or in its two copies in the bridge, is termed the EPG phase (e.g., 0° and 90° in **Figure 2*b***).

Some initial observations were key to understanding the EPG signal. (*a*) When a fly was presented with a prominent, distant visual cue in a virtual environment, such as a tall blue bar, the EPG phase closely tracked the cue's angular position, without drift (Seelig & Jayaraman 2015). (*b*) The alignment between the cue and the EPG phase varied across flies. For example, in one fly the bump might be at the top of the ellipsoid body when the cue is directly in front, whereas in another it might be at the bottom or on the side. This offset was generally stable but occasionally changed even within a single fly. Such flexibility ruled out the EPG phase being a simple visual signal in retinal coordinates (Seelig & Jayaraman 2015). (*c*) Supporting this conclusion, the bump persisted and rotated with the fly's turns, even in complete darkness. In darkness, however, the phase gradually drifted relative to the fly's orientation in the virtual environment, suggesting that the fly integrates its turns with accumulating error in the absence of visual input (Seelig & Jayaraman 2015, Green et al. 2017, Turner-Evans et al. 2017). (*d*) When EPG neurons were stimulated in one location around the ring, the bump invariably disappeared from its previous location while reappearing at the stimulated one (Green et al. 2017, Kim et al. 2017).

These observations indicated that the EPG bump arises from a winner-take-all network whose properties resemble ring-attractor models that have been applied to the mammalian head-direction system (Amari 1977, Ben-Yishai et al. 1995, Skaggs et al. 1995, Redish et al. 1996, Sharp et al. 1996, Zhang 1996, Green & Maimon 2018, Hulse & Jayaraman 2020, Fisher 2022, Wilson 2023). By analogy, the EPG phase thus seemed poised to track a fly's heading or head direction. This interpretation was solidified by studying the EPG system in the context of a behavioral task. Head-fixed *Drosophila* will walk (Green et al. 2019) or fly (Giraldo et al. 2018) along an arbitrarily chosen goal angle for hundreds or thousands of body lengths. This behavior, called menotaxis (Heisenberg & Wolf 1984), is most clearly observed when flies are motivated to disperse, like when they are hot or hungry (Coyne et al. 1982, Green et al. 2019, Leitch et al. 2021). Silencing EPG activity was shown to strongly impair menotaxis (Giraldo et al. 2018, Green et al. 2019). Moreover, when flies were virtually rotated as they performed menotaxis, thus briefly dissociating their goal and compass angles, the EPG phase rotated with the turn, tracking the compass and not the goal angle (Green et al. 2019) (**Figure 2*c***). Even in complete darkness, flies would use the EPG phase as a compass signal to perform menotaxis with no visual feedback (Green et al. 2019).

Collectively, these results established the EPG phase as an internally generated compass signal. Specifically, the EPG phase indicates the orientation of a fixed direction in the external world relative to the fly, analogous to a compass needle pointing north. As a result, EPG cells are sometimes called compass neurons. It is equally valid to view the EPG phase—which rotates in the brain when the fly turns—as tracking the orientation of the fly relative to a fixed direction in the external world. This variable is commonly called the fly's heading or head direction.[3] The compass and heading angles differ only by a sign. Because EPG neurons innervate 16 discrete wedges in the ellipsoid body, a natural assumption is that the resolution of the EPG compass is 22.5° (i.e., 360°/16). In reality, the EPG bump seems capable of residing stably at intermediate positions between neighboring wedges (Seelig & Jayaraman 2015, Green et al. 2017), meaning that the angular resolution of this system is higher than 22.5°, approximating something closer to a continuous ring (Noorman et al. 2024).

[3]Because published physiological measurements have only been made with head and body fixed to each other, it is unclear whether the EPG phase tracks head direction or body heading (though head direction seems likely).

How is the EPG phase determined? In particular, how does the system integrate the fly's turns to update the phase (e.g., in darkness) and, in addition, use sensory cues that are informative about the fly's orientation to yoke the phase when such cues are available? Neural circuits for both of these computations have been described (Green et al. 2017; Turner-Evans et al. 2017, 2020; Fisher et al. 2019, 2022; Kim et al. 2019, Hulse et al. 2021, Garner et al. 2024) (**Figure 2*d*,*e***).

To update the EPG phase by angular velocity integration, flies use a recurrent circuit between EPG cells and protocerebral bridge–ellipsoid body–nodulus (PEN) cells (Wolff et al. 2015; Green et al. 2017; Turner-Evans et al. 2017, 2020; Hulse et al. 2023). PEN neurons receive EPG input in the protocerebral bridge and project back to the ellipsoid body, offset slightly clockwise or counterclockwise relative to their input (**Figure 2*d***, left). At rest, left- and right-bridge PENs are equally driven by the EPG bump (**Figure 2*d***, left). During a left turn, left-bridge PENs become more active, shifting the bump clockwise; right turns produce the opposite effect (**Figure 2*d***, center and right). In Marr's (1982) framing, the computation being implemented is angular velocity integration; the algorithm being used is a three-ring shift circuit (Skaggs et al. 1995, Zhang 1996); and the implementation is the EPG/PEN feedback loop, where a single EPG ring in the ellipsoid body interacts recurrently with one PEN ring in the left bridge and a second PEN ring in the right bridge. The system is tuned so that the EPG phase rotates at a velocity that matches the fly's angular velocity, but, like all integrators, it is prone to drift. This fact necessitates a more reliable mechanism for updating the EPG phase, one based on cues that directly inform the fly of its orientation without the need for integration.

To update the EPG phase via direct sensory evidence of the compass angle, flies make use of tangential neurons of the ellipsoid body, also known as ring neurons (Hanesch et al. 1989, Omoto et al. 2017, Hulse et al. 2021, Garner et al. 2024) (**Figure 2*e***). Each ring neuron receives sensory input outside the central complex and projects an axon that encircles the ellipsoid body, contacting all EPG cells. These neurons are typically inhibitory (Hanesch et al. 1989, Fisher et al. 2019) and have spatially localized, visual receptive fields (Seelig & Jayaraman 2013). When a fly faces a given direction, a specific subset of ring neurons is activated by the current visual scene, coinciding with an EPG bump at some position in the ellipsoid body. A plasticity process then weakens the inhibitory effect of the currently active ring neurons on the currently active EPG cells. As the fly turns, the PEN system shifts the EPG bump via angular integration, and the newly active EPG cells undergo the same plasticity with newly coactive ring neurons. Over minutes, this learning procedure creates a map such that viewing familiar visual scenes can reposition the EPG bump appropriately (Fisher et al. 2019, Kim et al. 2019) (**Figure 2*e***). Airflow-sensitive ring neurons can also stabilize the EPG bump, which is helpful when wind arrives from a reliable direction and visual information is poor (Okubo et al. 2020, Siliciano et al. 2025). Likewise, patterns of polarized light in the sky, to which certain ring neurons are tuned, are also poised to align the EPG compass (Hardcastle et al. 2021, Hulse et al. 2021, Garner et al. 2024). Overall, the compass system appears to dynamically weigh input from neurons informative about the rate change of heading (PENs) as well as the absolute heading (ring neurons), promoting the impact of the most reliable cues at any given time on the EPG phase (Hulse et al. 2021, Fisher 2022, Mitchell et al. 2023, Wilson 2023, Basnak et al. 2025, Ishida et al. 2025).

## Beyond the Compass: Vector Computations in the Fan-Shaped Body

The compass angle indicated by the EPG phase is a key anchor signal from which the fly constructs its allocentric understanding of space, and this understanding relies on, in large part, computations within the fan-shaped body. Anatomically, the two axonal copies of the EPG bump in the bridge are poised to drive bumps in over a dozen downstream columnar neuron populations, whose dendrites

also tile the bridge (Wolff et al. 2015, Hulse et al. 2021). As will be explained below, the structure of these recipient bumps allows them to be treated as mathematical vectors. The angle of each vector, when measured in the bridge, tracks the EPG phase angle, and its length is regulated by other factors. Many of these columnar cell classes in the bridge project to the fan-shaped body, where the vectors they encode are rotated, added, and multiplied to implement computations needed for navigation. Sensory information and contextual inputs modulate these vector operations, flexibly adapting them to the flies' current behavioral needs.

Akin to the circular ellipsoid body and the two sides of the protocerebral bridge, the fan-shaped body is also functionally circular, with activity between its left and right edges mapping to 360° around the fly (**Figure 1*e***). All of these effective circles can be parameterized across their spatial extent by an angle, and these angles can be aligned to those of the ellipsoid body by examining the interconnectivity between regions (Hulse et al. 2021, Lyu et al. 2021). This fact has important implications for the study and function of the central complex. For researchers, it greatly facilitates the interpretation of both the anatomy and imaged activity. For example, the proper geometry for visualizing and interpreting population-level neural signals is largely determined by the spatial organization of neurons within the system, making the dimensionality-reduction techniques commonly used in other animal models unnecessary. For the flies, the angular alignment between the ellipsoid body, bridge, and fan-shaped body has many computational benefits, such as allowing angular and vector rotations to be performed anatomically by spatially shifting axonal projections. To understand why this is the case, we first need to describe how the central complex encodes vectors.

Vectors can be specified as a direction and length or, alternatively, as a list of coordinates that define the projections of the vector onto a set of axes (Arianrhod 2024). At the level of the activity of individual neurons, the central complex encodes vectors as a set of coordinate values. Specifically, when the EPG phase signal is transmitted to columnar neurons in the bridge, it is transformed into a vector pointing in the direction of the EPG phase, with the activity of single downstream cells expressing that vector's coordinates (Stone et al. 2017, Hulse et al. 2021, Lyu et al. 2021). However, these coordinates differ from the conventional Cartesian ones (**Figure 3*a***, top) in two fundamental ways. First, rather than encoding only the usual $x$ and $y$ coordinates, the representation explicitly includes $x$ and $y$ and $-x$ and $-y$ as four separate axes. Second, there are four more axes, tipped from the first four by 45°. Thus, in total, vectors in the bridge are characterized by eight rather than two numbers (**Figure 3*a***, bottom). These coordinates, which are encoded by the activity levels of neurons in the different bridge glomeruli (one glomerulus per coordinate), are computed by a set of interneurons that tile the bridge called Delta-7 (Δ7) cells (Wolff et al. 2015, Hulse et al. 2021, Lyu et al. 2021). Each Δ7 neuron receives the compass signal from the entire EPG population through a set of synapses whose density varies sinusoidally across the bridge (Wolff et al. 2015, Hulse et al. 2021). This sinusoidal connectivity profile causes the activity of single Δ7 cells to track the projection of a unit vector pointing in the EPG direction onto one of the 8 axes just described. The full array of Δ7 cells computes the relevant eight projections and transmits them to various arrays of downstream neurons (described below) in eight glomeruli in the left bridge and eight glomeruli in the right bridge, in duplicate (Lyu et al. 2021).

If the eight coordinates we have been discussing are plotted across glomeruli, they trace out a sinusoidal shape. Thus, at the population level, the activity of each set of columnar neurons downstream of the EPG signal forms two sinusoidal bumps across the bridge, one on each side (Green et al. 2017, Lyu et al. 2021) (**Figure 3*b***). Each of these bridge sinusoids can be considered a phasor representation of a vector, where the peak position of the sinusoid encodes the vector's angle and the amplitude encodes its length (O'Keefe 1991, Touretzky et al. 1993, Hartmann & Wehner 1995, Wittmann & Schwegler 1995, Stone et al. 2017, Lyu et al. 2021). Because the peak

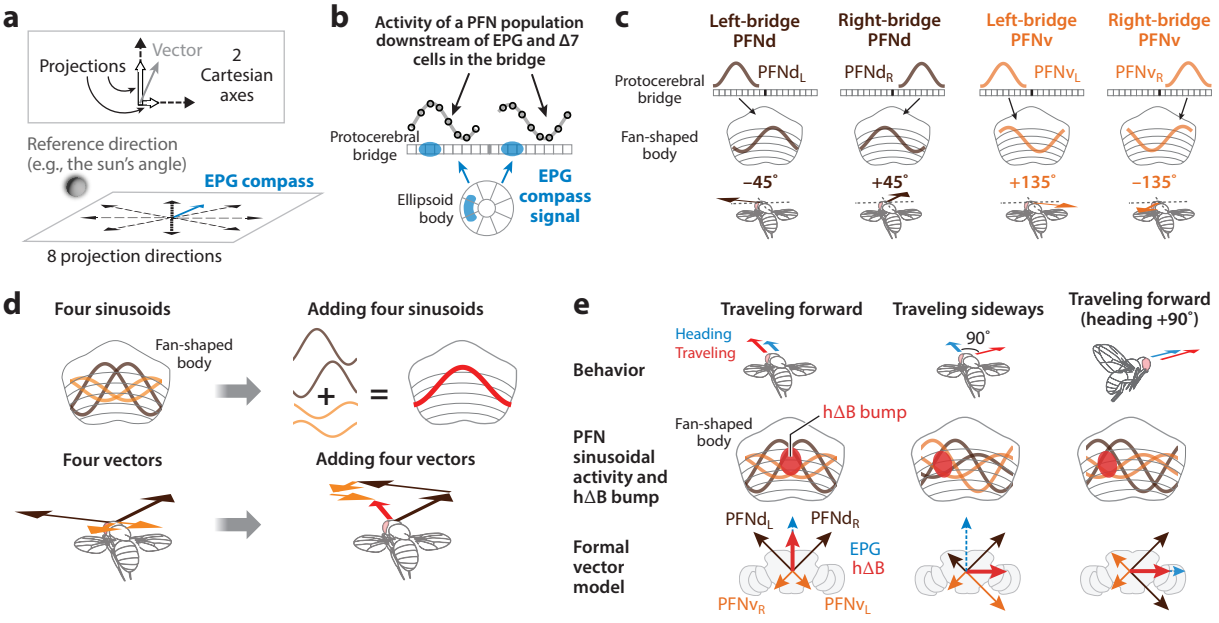


**Figure 3**

PFN neurons perform an egocentric-to-allocentric coordinate transformation via vector computation. (*a*, *top*) In a conventional 2D Cartesian system, vectors are projected onto two orthogonal axes, generating two coordinates. (*Bottom*) PFN neurons use an overcomplete system in which vectors are projected onto eight axes that are separated by 45°. These axes are locked to fixed directions in the world by the EPG compass, making them an allocentric system. (*b*) Δ7 neurons compute projections of the EPG compass vector onto the eight axes shown in panel *a*. Collectively, these eight projections yield sinusoidal patterns of activity (i.e., phasors) in the PFN neurons of the bridge, which are monosynaptically downstream of EPG and Δ7 cells. Each PFN class expresses two vector-encoding phasor signals: one in the left bridge, and a second in the right bridge. When a fly turns, the EPG bump and the PFN phasors it drives in the bridge counter-rotate in unison. (*c*) The dendrites of PFNd neurons (*brown*) and PFNv neurons (*orange*) each express two phasors in the bridge. These cells send axons to the fan-shaped body, and the anatomy and physiology of these projections lead the PFNd and PFNv phasors to be functionally shifted by the angles indicated. The result is four phasors or vectors in the fan-shaped body pointing at +45°, −45°, +135°, and −135° relative to the EPG angle or the fly's heading. (*d*) Each PFNd and PFNv phasor encodes a single 2D vector, and a vector sum operation is performed across these four sinusoids or vectors in the fan-shaped body. When one sums four PFNd and PFNv sinusoids (*brown* and *orange curves*), a new sinusoid is generated (*red curve*). This sinusoid-summing process is equivalent to performing vector addition on the four PFNd and PFNv vectors encoded by the sinusoids (*brown* and *orange arrows*), thus generating a summed, or resultant, vector (*red arrow*). (*e*) hΔB cells sum the PFNd and PFNv sinusoids, with this summed vector signal tracking the fly's traveling direction in allocentric coordinates. (*Left*) When the fly travels forward (i.e., along its heading angle), the two PFNd sinusoids (*brown*) grow in amplitude and the two PFNv sinusoids (*orange*) shrink, such that their sum yields a sinusoid—signaled by hΔB neurons—with a peak position or phase (*red dot* and *red arrow*) that aligns with the fly's heading (*blue arrow*). (*Middle*) When the fly travels sideways relative to its heading, one PFNd and one PFNv sinusoid grow, and the other pair shrinks, such that their sum yields an hΔB sinusoid with a peak position or phase offset 90° from the EPG signal. (*Right*) When the fly turns 90°, the EPG signal rotates the whole reference frame. If the fly travels forward in this new, rotated reference frame, the summed hΔB sinusoid captures the same allocentric traveling direction as in the middle panel by summing the PFN vectors. Panels *c* and *e* adapted with permission from Lyu et al. (2021).

position of each bridge sinusoid slides along the bridge when a fly rotates, tracking the EPG phase, each bridge vector points in the EPG-encoded direction. The amplitude of each sinusoid (i.e., the vector's length) is regulated by other factors, described below. The phasor framework describes vector signals in a compact polar (angle and length) form (Touretzky et al. 1993); however, it is important to note that the encoding scheme of this system, at the level of single-neuron activity, is that of a Cartesian-like representation, which has advantages over a polar encoding for performing low-noise vector operations (Vickerstaff & Cheung 2010).

In what follows, we first describe how the EPG-yoked vectors in the bridge allow this system to place egocentric sensory input into an allocentric reference frame within the fan-shaped body. We then describe how an allocentric goal signal in the fan-shaped body can be transformed back into an egocentric form to drive steering. It is possible to describe both these computations in the language of vector coordinates (see the Appendix). Indeed, such a description may prove helpful for the study of mammalian navigational signals where many single cells can be recorded at a time but where visualizing entire, functionally unified, cell populations is not as straightforward as it is in the central complex. In *Drosophila*, however, where modern imaging approaches allow experimenters to comprehensively measure the activity of all the constituent members of most columnar cell classes, and where those cells are arrayed anatomically in a favorable manner for interpreting their activity, we opt for the population-level, phasor-based description of function in the following text.

## An Allocentric Traveling Direction Signal in the Fan-Shaped Body

Flying insects determine the direction and speed at which they are traveling in the world by analyzing the global pattern of visual motion, or optic flow, on their retinas (Krapp 2000, Mauss & Borst 2020, Henning et al. 2022, Egelhaaf 2023, Zhao et al. 2025). If a fly is attempting to fly straight in the context of a crosswind, its traveling direction as revealed from optic flow will not necessarily coincide with its heading direction, that is, the direction in which the head or body is pointing. To calculate their traveling direction in an allocentric coordinate frame, flying flies make use of their EPG heading direction signal alongside a set of visual optic flow–tuned inputs, as follows.

The visual processing of optic flow culminates in the activity of four sets of neurons that receive inputs outside the central complex and project to the noduli. These neurons report the projections of the fly's egocentric traveling vector (as estimated by optic flow) onto four directions tilted ±45° and ±135° relative to the fly's head. In the noduli, this information is conveyed to two types of columnar neurons: protocerebral bridge–fan-shaped body–nodulus-compartment-2-dorsal-aspect (PFNd) cells, and protocerebral bridge–fan-shaped body–nodulus-compartment-2-ventral-aspect (PFNv) cells. **Figure 1*c*** (bottom left) shows a schematic of a single PFN neuron. PFNd and PFNv neurons integrate their nodulus inputs conveying the fly's egocentric traveling vector with their bridge inputs from the EPG/Δ7 system, and they transmit the combined signal to the fan-shaped body via their axonal outputs. Across the bridge, both PFNd and PFNv cells express a pair of phasors (as described above) that represent four parallel vectors, all pointing in the same, EPG-defined direction. This degeneracy is broken by their pattern of axonal projections from the bridge to the fan-shaped body. PFNd neurons with dendrites innervating the left bridge ($PFNd_L$ cells) project axons to the fan-shaped body with a −45° offset, while those innervating the right bridge ($PFNd_R$ cells) express a +45° offset. As a result, the sinusoidal patterns of PFN activity in the fan-shaped body no longer represent two parallel vectors tied to the compass, but two axes of an orthogonal coordinate system tied to the compass. This forms the basis for representing the egocentric traveling vector in an allocentric coordinate system (**Figure 3*c***). The left and right PFNv neurons (i.e., $PFNv_L$ and $PFNv_R$ cells) have effective shifts of ±135°, so they provide an orthogonal basis oriented in the reversed direction from that of the PFNd neurons (**Figure 3*c***).[4] Together, the PFNd and PFNv neurons thus construct a four-axis Cartesian coordinate system.

[4]The ±45° and ±135° PFNd and PFNv basis-vector angles are achieved as follows. The axonal projections of PFNd and PFNv cells from the bridge to the fan-shaped body are actually quite similar. Nevertheless, we

The next step in building an allocentric traveling direction signal is to project the fly's egocentric traveling vector (estimated via optic flow)—which, recall, takes the form of projections onto four egocentric axes—onto the four allocentric axes defined by the left and right PFNd and PFNv cells in the fan-shaped body. Specifically, the effect of the optic flow input is to modulate the amplitude of the four PFNd and PFNv phasors (**Figure 3*d***). Because the amplitude of a phasor encodes the length of a vector, this amplitude modulation corresponds to multiplying each PFN basis vector by the value of its corresponding coordinate. The result of summing the four PFN sinusoidal activity patterns, which is equivalent to summing four length-modulated basis vectors, is a vector that points in the allocentric traveling direction of the fly (**Figure 3*d***). Remarkably, this vector sum is performed by hDeltaB (hΔB) neurons, which are monosynaptic recipients of PFNd and PFNv input in the fan-shaped body (**Figure 3*e***). The hΔB activity pattern represents the allocentric traveling direction vector as a phasor, or equivalently, individual hΔB cells provide an eight-component encoding of traveling direction in the fan-shaped body, analogous to that for compass direction in the bridge. Consistent with this framing, experimental results show that the phase of the fan-shaped body bump in hΔB neurons indeed tracks the allocentric traveling angle of the fly (Lu et al. 2021, Lyu et al. 2021), and experimentally lengthening or shortening the PFNd or PFNv vectors has the predicted effect on the hΔB readout (Lyu et al. 2021). The same computation is performed in walking flies, but with a greater reliance on proprioceptive or efference copy–based estimates of the egocentric traveling vector over visual optic flow (Lu et al. 2021, Lyu et al. 2021).

At Marr's (1982) first level, this system performs a transformation from a coordinate system that is fixed to the fly's head (egocentric) to a coordinate system that is fixed to the world (allocentric). At Marr's second level, this transformation is achieved by projecting sensory information in the egocentric frame onto four allocentric directions defined by ±45° and ±135° rotations of a compass direction. At Marr's third level, these computations are performed by exploiting a combination of anatomical and physiological features of EPG, Δ7, PFNd, PFNv, and hΔB cells (Lu et al. 2021, Lyu et al. 2021) (see the Appendix).

## Steering Output of the Fan-Shaped Body

As just described, the fly's traveling direction is converted from egocentric to allocentric coordinates by PFNd and PFNv neurons. Parallel sets of PFN neurons are poised to similarly transform other variables of relevance from egocentric into allocentric coordinates (Wolff et al. 2015, Hulse et al. 2021). For example, the allocentric direction of wind, a notoriously challenging vectorial computation for flying insects (Leitch et al. 2021, Van Breugel et al. 2022, Stupski & Van Breugel 2024), may be determined by an analogous process (though with interesting differences as well) (Currier et al. 2020, Ishida et al. 2025, May et al. 2025). Using an array of allocentric vectors tracking environmental angles of relevance, flies are poised to construct a spatial understanding of their world. Using this spatial understanding, the fly ultimately needs to build a goal direction along which it wishes to travel and a mechanism to orient itself along that direction.

We have already mentioned one goal-directed navigation task, menotaxis, that relies on the central complex (**Figure 2*c***). Other tasks that allow the experimenter to flexibly promote specific

consider the system to be functionally rotating the PFNd and PFNv vectors quite differently: ±45° for PFNd cells and ±135° for PFNv cells. This 180° difference arises from the manner in which PFNd and PFNv cells synapse onto their readout neurons, hΔB cells, in the fan-shaped body. PFNd cells synapse preferentially on the axon terminals of hΔB neurons within a given fan-shaped body column, whereas PFNv cells target the hΔB dendrites in a given column. Because hΔB cells have a 180° offset between their dendritic and axonal terminals in the fan-shaped body, this adds 180° to the functional offset of PFNv phasors compared to PFNd phasors in regard to their impact on the hΔB readout signal.

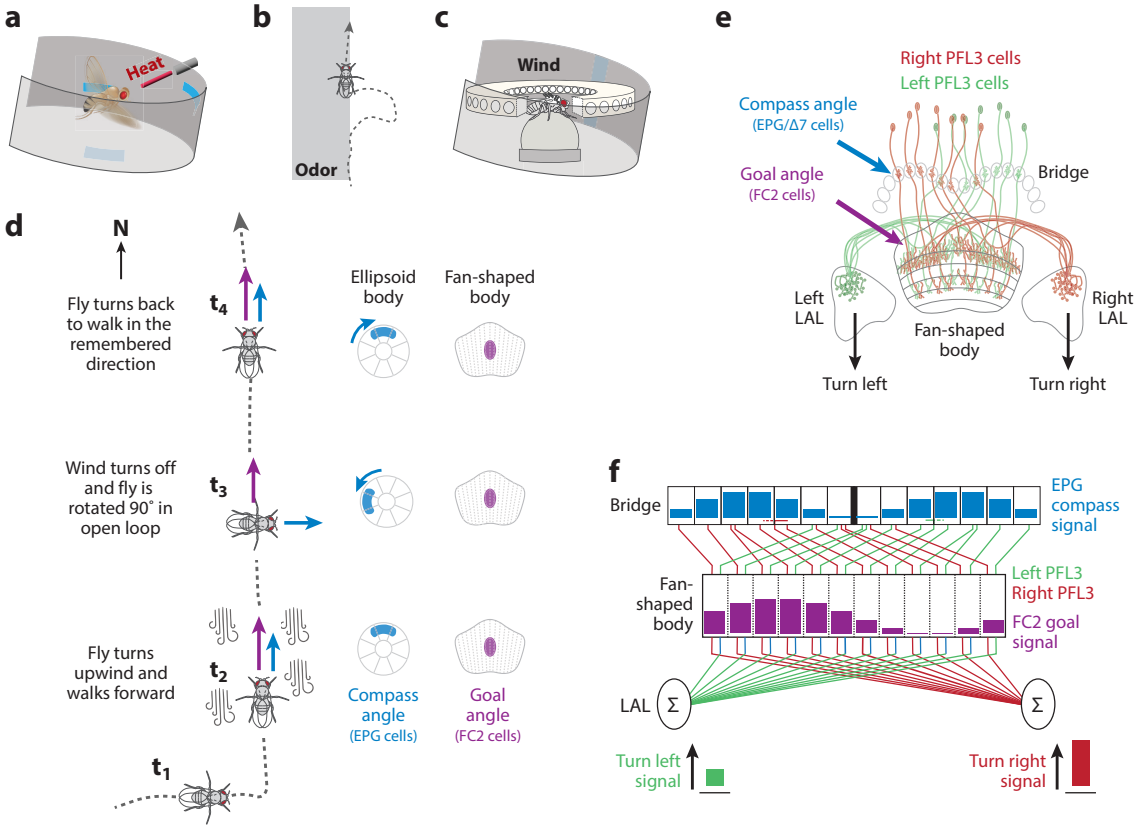


**Figure 4**

The output of the central complex implements an allocentric-to-egocentric coordinate transformation to drive goal-directed turning. (*a*) Heat-induced working memory task (Dan et al. 2024). Tethered, flying flies remember a direction associated with heat avoidance in a virtual environment. (*b*) Odor edge-tracking task (Siliciano et al. 2025). Tethered, walking flies loop away and back to an odor plume using the central complex. (*c*) Wind-induced working memory task (Mussells Pires et al. 2024). Flies remember an allocentric wind direction for seconds to minutes after the wind turns off. (*d*) Time progression of the wind-induced working memory task schematized in panel *c*. EPG cells track the fly's heading or compass angle, and FC2 cells track the fly's goal angle. (*e*) PFL3 neurons receive monosynaptic compass inputs from EPG and Δ7 cells in the bridge. They also receive monosynaptic goal inputs from FC2 (and other) cells in the fan-shaped body. These two signals are in allocentric coordinates. Because 12 of 24 PFL3 cells project axons to the left LAL and the other 12 to the right LAL, and the two LALs are premotor regions associated with driving locomotor turns, the differential output between the left and right PFL3 cells is poised to generate an egocentric steering signal that promotes turning toward the goal angle. (*f*) Schematic of the 24 PFL3 cells. Blue bars show the activity of EPG cells in the bridge, where the EPG compass signal exists as two bumps. Purple bars show the single bump of FC2 activity in the fan-shaped body. Red and green lines represent the neurites of PFL3 cells. Individual PFL3 cells sum a compass input that they receive from one glomerulus in the bridge with a goal input that they receive from one column of the fan-shaped body, while projecting their axonal output to either the right LAL (*red PFL3 cells*) or left LAL (*green PFL3 cells*), which are premotor regions associated with locomotor turns. The scenario depicted in this panel is one where the FC2 goal angle is to the right of the fly's current heading, leading more red PFL3 cells to have strong EPG and FC2 joint input compared to green PFL3 cells, yielding a larger summed PFL3 output in the right LAL compared to the left LAL, thus creating a motivation for the fly to turn right. Panels *e* and *f* adapted with permission from Mussells Pires et al. (2024) (CC BY 4.0).

allocentric goal angles over others have since come online (**Figure 4*a–c***). For example, flies can learn to avoid directions associated with heat (Wolf & Heisenberg 1991, Dan et al. 2024) (**Figure 4*a***), navigate along a virtual odor plume (Siliciano et al. 2025) (**Figure 4*b***), or remember a recently experienced wind direction (Mussells Pires et al. 2024) (**Figure 4*c***). Performance of all of

these tasks is impaired by silencing the EPG compass (Dan et al. 2024, Mussells Pires et al. 2024, Siliciano et al. 2025). In the wind-induced memory task (Mussells Pires et al. 2024) (**Figure 4*c*,*d***), head-fixed flies walking in a virtual environment innately turn to walk upwind when a closed-loop wind stimulus is turned on (**Figure 4*d***, bottom). When the wind is turned off and the fly is virtually rotated away from the just-experienced upwind direction (**Figure 4*d***, middle), the fly rotates back to the remembered direction of the wind and walks forward along this direction for many seconds to minutes (**Figure 4*d***, top). In other words, flies can remember a recently experienced upwind direction even after the wind dies down. They are completely incapable of forming or expressing such a memory if their EPG compass is silenced (Mussells Pires et al. 2024).

These results point toward angular memories that are stored in allocentric coordinates. Indeed, a set of columnar neurons in the fan-shaped body, called fan-shaped body–crepine–type-2 (FC2) cells (Hulse et al. 2021), express a bump of activity that does not rotate when flies are virtually rotated off of their goal direction (Mussells Pires et al. 2024) (**Figure 4*d***). This observation, along with perturbation experiments in which the FC2 bump was experimentally repositioned in the fan-shaped body (Mussells Pires et al. 2024), strongly argues that the FC2 bump signals a goal angle, which is poised to be compared with the EPG compass angle to drive turns.

Because the goal is encoded in allocentric coordinates, for the system to generate a goal-directed steering signal, this information must be transformed back into egocentric coordinates appropriate for controlling the body. This means, essentially, undoing the transformation that was done at the input stage by PFN neurons. For steering, this computation is performed by protocerebral bridge–fan-shaped body–lateral accessory lobe–type 3 (PFL3) cells (Stone et al. 2017, Hulse et al. 2021, Matheson et al. 2022, Goulard et al. 2023, Mussells Pires et al. 2024, Westeinde et al. 2024).

Single PFL3 neurons receive inputs in both the protocerebral bridge and fan-shaped body and send an axonal output to either the left or right lateral accessory lobe, or LAL (**Figure 4*e***). The LALs are premotor structures flanking the central complex that control locomotion speed and turning (Iwano et al. 2010, Schnell et al. 2017, Namiki et al. 2022, Braun et al. 2024, Feng et al. 2024, Yang et al. 2024, Rayshubskiy et al. 2025). This system converts an allocentric goal into an egocentric steering signal as follows. Each PFL3 neuron receives compass-related input from EPG and Δ7 neurons within one glomerulus in the bridge and goal-related input from FC2 neurons in one column of the fan-shaped body (Hulse et al. 2021) (**Figure 4*e*,*f***). At the population level, the compass and goal signals that provide input to PFL3 cells take the form of three phasors or vectors. In **Figure 4*f***, the blue bars indicate the coordinate values of the compass-aligned vector, and the purple bars indicate the coordinate values of the goal-aligned vector, with the shapes outlined by the tops of the bars delineating the corresponding phasors. There are 24 total PFL3 cells, pairs of which project from two different glomeruli in the bridge to a common column in the fan-shaped body (**Figure 4*f***), and in that column, the pair receives a common goal-related input from FC2 neurons. At the level of their membrane voltage, PFL3 neurons simply sum their compass and goal inputs (Mussells Pires et al. 2024), but the nonlinearity of their voltage-to–spike rate function effectively multiplies these signals to compute vector products (Mussells Pires et al. 2024). One of the pair of PFL3 neurons innervating a given fan-shaped body column sends an axon to the right LAL (to promote right turns), and the other projects to the left LAL (to promote left turns). The output signals carried by all the left-LAL-projecting and right-LAL-projecting PFL3 cells are summed in the LALs, and the difference between the left and right sums defines the egocentric turning signal (Mussells Pires et al. 2024, Westeinde et al. 2024). The steering signal, which takes the form of a sine function of the difference between the goal and heading angles, matches both neural recordings and behavioral measurements (Green et al. 2019, Mussells Pires et al. 2024). A

sister set of PFL2 neurons contributes in a nondirectional manner to overall turn vigor when the fly is oriented very far away from its desired goal direction (Westeinde et al. 2024).

In this system, the description at Marr's (1982) first level is the computation of an egocentric steering signal that causes a fly to turn toward a desired goal direction, with the goal angle generated internally and not necessarily based on any currently experienced stimulus. The most pithy description at Marr's second level is that the system computes a scalar cross product between compass-aligned and goal-aligned vectors to generate the appropriate steering signal (see the Appendix). In this circuit, patch-clamp electrophysiological recordings have revealed both how PFL3 neurons sum their compass and goal inputs and how they nonlinearly transform (effectively multiply) these inputs via their voltage-to–spike rate nonlinearity (Mussells Pires et al. 2024). Such electrophysiological measurements, alongside calcium imaging experiments, behavioral experiments, and EM-level analyses of the connectivity between EPG, FC2, and PFL3 neurons, provide a detailed explanation, at Marr's third level, of how the steering algorithm is implemented.

## CONCLUSIONS AND OUTLOOK

### Memory and Integration in the Fan-Shaped Body

Marr's (1982) levels have achieved alignment for several real-time signals in the *Drosophila* central complex, including the EPG compass and hΔB traveling direction bumps, and for circuits underlying coordinate transformations. These elements in the system have come into focus first, at least in part, because their explanations hinge on patterns of connectivity revealed by the connectome. Understanding state-dependent computations and how spatial memories are built, stored, and read out, questions that are now at the frontier, will require further improved behavioral tasks and delving deeper into the biochemistry of neurons, transcending the connectome.

Inspiration for how spatial memories could manifest in the fly central complex has arisen from the study of ants and bees (von Frisch 1967, Hartmann & Wehner 1995, Wittmann & Schwegler 1995, Stone et al. 2017, Wehner 2020, Goulard et al. 2023). These insects path integrate their traveling vector during foraging excursions to build a home vector (von Frisch 1967, Wehner 2020). The home vector has been modeled as a phasor in the fan-shaped body (Hartmann & Wehner 1995, Wittmann & Schwegler 1995, Stone et al. 2017, Goulard et al. 2023). By analogy, spatial memories in *Drosophila*, such as remembering the allocentric wind direction after the wind disappears, are also likely to be phasor signals in the fan-shaped body (Hulse et al. 2021, Matheson et al. 2022, Goulard et al. 2023, Dan et al. 2024, Kathman et al. 2024, Mussells Pires et al. 2024, Siliciano et al. 2025, Westeinde et al. 2024). Indeed, *Drosophila* might even perform a rudimentary form of path integration to build vector memories (Kim & Dickinson 2017, Corfas et al. 2019, Behbahani et al. 2021, Lu et al. 2021, Titova et al. 2023, D'Atri & DasGupta 2025).

Thus, we imagine that a fly standing on a rotten fruit keeps track not only of real-time navigational variables such as the EPG compass direction but also of memory directions of interest in allocentric coordinates (**Figure 5*a***). Each memory direction may be stored as a phasor across a population of fan-shaped body columnar neurons (**Figure 5*b***, top). Because phasor-based vector memories need to be stored for minutes, hours, or days (Ziegler & Wehner 1997, Pisokas et al. 2022), a variety of mechanisms with differing persistence times may be involved (**Figure 5*b***, bottom). Revealing these mechanisms is likely to impact the broader field of learning and memory, because we should be able to articulate, explicitly, what an angular memory looks like in a brain: a sinusoidally varying synaptic weight profile across a columnar population, for example. Critically, we will also be able to test whether this idea is correct by experimentally manipulating the sinusoidally varying variable to show that the memory shifts to a different, quantitatively predictable angle based on which column in the fan-shaped body expresses the peak value. Ten or

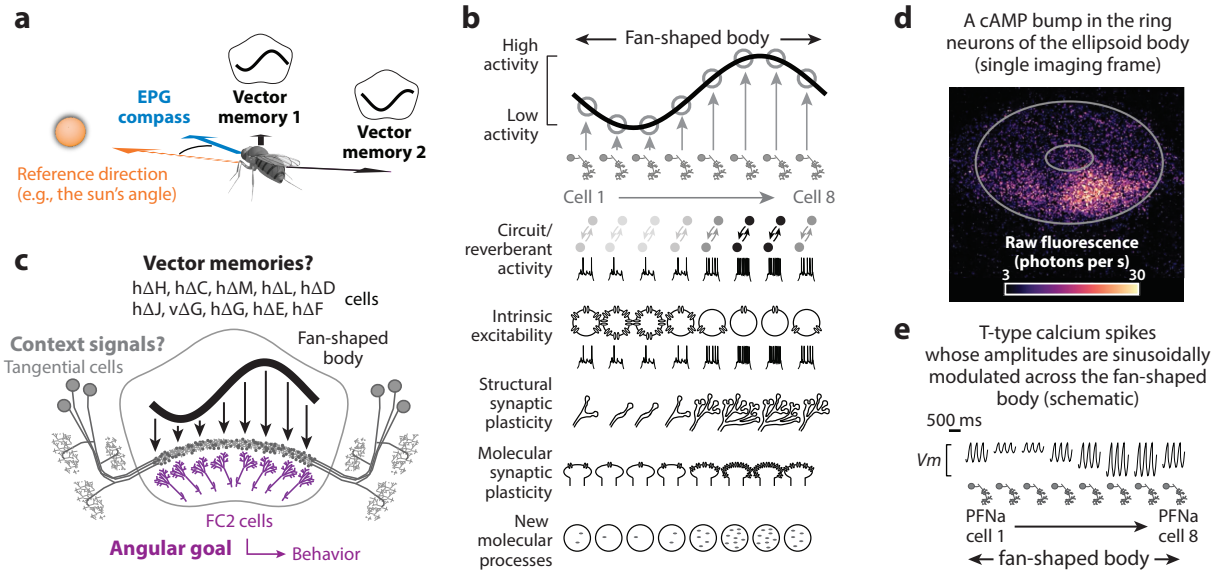


**Figure 5**

Vector memories in the fan-shaped body and potential mechanisms for storing them. (*a*) A fly with two hypothetical vector memories in the fan-shaped body, each pointing in a different direction and each expressed as a sinusoidal activity pattern or phasor. (*b*) Potential mechanisms for storing a vector memory as a phasor in columnar cells of the fan-shaped body. (*c*) Vector memory signals are putatively stored as phasors in columnar cells that provide monosynaptic input to FC2 cells. Tangential neurons are poised to contextually select which of the memory phasors are passed on to the FC2 cells at any given moment to guide behavior. (*d*) Preliminary recordings employing green fluorescent cAMP indicator 1 (G-Flamp1) (Wang et al. 2022) in ring neurons of the ellipsoid body reveal a cAMP bump of activity in their axons, which fundamentally determines how visual information is transmitted to EPG cells, thus anchoring the compass sense to the external world. Image in panel *d* from unpublished data collected by Stephen Thornquist (Maimon lab). cAMP-regulated processes are poised to similarly impact the physiology of columnar cells in the fan-shaped body to aid the building of vector memories. (*e*) Protocerebral bridge–fan-shaped body–nodulus compartment 3 anterior aspect (PFNa) columnar cells in the fan-shaped body fire T-type calcium spikes whose amplitude is sinusoidally modulated across the fan-shaped body, encoding a vector (Ishida et al. 2025). These spikes are poised to contribute to vector memories. Traces shown in this panel are schematics, not actual data.

more columnar populations in *Drosophila* provide monosynaptic input to the FC2 system (Hulse et al. 2021). Each of these could contribute toward storing vector memories of different durations and under different conditions (**Figure 5*c***). Tangential cells that are interposed between these columnar populations and the FC2 goal population are poised to contribute toward generating vector memories, uploading them from memory, and/or selecting which one is allowed to influence the FC2 goal signal at any given moment (**Figure 5*c***). Many tangential neurons release monoamines and/or neuropeptides that could regulate such computations.

Identifying the cell populations that store vector memories should enable discovery of the biochemical and biophysical mechanisms that implement these memories (**Figure 5*b***). For example, imaging second messengers, such as cAMP (Liu et al. 2022), in genetically defined cell types is fast becoming routine. Our own preliminary imaging experiments in ring neuron axons have revealed a rotating cAMP bump that serves a critical role in determining whether visual patterns are learned by the EPG compass (**Figure 5*d***). This cAMP signal likely relies on the presynaptic release of monoamines (Plitt et al. 2025) and/or neuropeptides. cAMP is likely to serve a similar role in forming vector memories in the fan-shaped body. In the fan-shaped body, a class of PFN neurons that uses T-type calcium spikes to perform vector operations has been described (Ishida et al. 2025) (**Figure 5*e***). These calcium spikes are poised to contribute to storing

or integrating phasors over time. In the dorsal fan-shaped body, neuronal excitability is strongly altered, for hours, via the addition or removal of specific $K^+$ conductances (Pimentel et al. 2016, Kempf et al. 2019, Hasenhuetl et al. 2024, Rorsman et al. 2025, Sarnataro et al. 2025). While ion channel modulation has thus far been linked primarily to the integration of sleep pressure, similar mechanisms could underlie the integration of navigational information. *Drosophila* is an ideal system in which to relate such molecular processes to their computational roles in the brain.

## The Role of Symmetry

Artificial neural networks operate through connections whose strengths are adjusted to properly combine signals working in tandem with nonlinear input-output functions that process those signals. While many types of nonlinearities can be used, once a specific nonlinearity is chosen and the network is trained, the network's behavior critically depends on a precise match between its connectivity and the chosen nonlinearity. The fly central complex also relies on connectivity and nonlinearities to perform the coordinate transformations described above, but the embedded symmetry in its architecture reduces the need for rigid cooperativity between these two elements. For most noninformative or spurious terms that arise from imperfect nonlinearities, the system includes a negative counterpart, canceling errors. This flexibility in handling nonlinearity imperfections may have allowed the connectivity and neuronal response properties of the central complex to coevolve without strict constraints, an evolutionary advantage that may have facilitated the emergence of the central complex.

## Further Frontiers

Beyond vector memories and understanding how symmetries might have enabled central complex evolution, many more mysteries remain. The fan-shaped body has been implicated in sleep (Donlea et al. 2011, Liu et al. 2016, Artiushin & Sehgal 2017; though see De et al. 2023), and how that function relates to navigation remains unclear. Insects navigate in 3D, yet most work has focused on 2D situations. Flies live for months, yet most work has focused on minutes-long signals and behaviors (though see Huang et al. 2018, Flores-Valle et al. 2022, Weisman et al. 2025). Perhaps most intriguingly, many of the outputs of the fan-shaped body connect not to motor circuits in the LAL but to deeper brain areas that feed back to the fan-shaped body via tangential neurons (Hulse et al. 2021), leaving a large fraction of the system's computations still awaiting discovery.

Might understanding the central complex have relevance outside of insects (Basu & Nagel 2024)? A remarkable recent advance is the discovery of head direction–like cells in the fish brainstem that resemble central complex neurons (Petrucco et al. 2023). The similarities include a calcium activity bump that rotates as the animal turns in a virtual world, with topographically arrayed neurites akin to fly columnar cells (Petrucco et al. 2023). If the history of genetics, development, and circadian biology has not already justified optimism that work in *Drosophila* can inform our understanding of vertebrates, these findings in the fish brainstem provide fresh, compelling support. Thus, there is increasing reason to believe that if the full set of methods used for studying fly navigation is ported to vertebrates, including mammals, a similar, multilevel understanding could materialize in those species as well.

## APPENDIX

Here we outline how the computations we discuss in the text can be understood from the standpoint of vector components rather than phasors. The projection of one vector onto another is given by their dot product. For example, if the compass angle $\theta_c$ is represented by a vector with components $[\cos\theta_c,\ \sin\theta_c]$, and the traveling direction angle, which we label $\theta_v$, is represented by $[\cos\theta_v,\ \sin\theta_v]$, their dot product $\cos\theta_v\cos\theta_c + \sin\theta_v\sin\theta_c = \cos(\theta_v - \theta_c)$ is the desired

projection. There are two major issues confronting a neural implementation of this computation. First, a neural response cannot easily represent a full sinusoidal function because it is typically constrained to be positive by virtue of neurons firing spikes only when depolarized. For the neurons we discuss, this is resolved by having the response equal to $A + B\cos\theta$ or $A + B\sin\theta$ with $A$ and $B$ chosen to avoid negativity. The second issue is that the dot product requires a multiplicative operation, but neurons do not typically multiply their inputs. This can be overcome by exploiting the nonlinearity of neural responses as a function of their inputs. For example, suppose a single PFN neuron received a compass input $A + B\cos\theta_c$ and a traveling direction input $A + B\cos\theta_v$, added them, and then responded with a squaring nonlinearity. This would produce the rather messy result $(A + B\cos\theta_c + A + B\cos\theta_v)^2$, which contains the desired product term $(\cos\theta_c\cos\theta_v)$ but also includes a number of other unwanted terms. However, each hΔB neuron sums the outputs from four PFN neurons, which we can write as $(A + B\cos\theta_c + A + B\cos\theta_v)^2$, $(A + B\sin\theta_c + A + B\sin\theta_v)^2$, $(A - B\cos\theta_c + A - B\cos\theta_v)^2$, and $(A - B\sin\theta_c + A - B\sin\theta_v)^2$. Summing these four terms gives the much neater result $A' + B'\cos(\theta_v - \theta_c)$, with $A' = 16A^2 + 4B^2$ and $B' = 4B^2$. This is, up to constants, exactly the needed dot product. The four responses being added here come from the left and right PFNd and PFNv neurons, and they are summed by hΔB neurons. The above result applies to one of the eight fan-shaped body columns innervated by the hΔB neurons. The same addition is done in the other columns, except that the compass signal is shifted by an angle $\varphi_i$ for column $i$, with this angle changing by 45° from one column to the next. The result is an eight-component representation of the traveling direction, $A' + B'\cos(\theta_v - \theta_c - \varphi_i)$ for $i = 1,\ldots, 8$, which forms a discrete representation of a phasor representing the traveling direction.

The calculation presented above gives the dot product answer because of cancelations that arise from a 90° rotation symmetry provided by the four-axis coordinate system used in the central complex. This symmetry has further implications as well. The dot product result obtained using a quadratic nonlinearity is a good approximation even if the response nonlinearity is not strictly quadratic, provided it does not deviate too far from this general shape. In other words, the circuit is configured so that unwanted terms arising from smooth, neuronal response nonlinearities automatically cancel, yielding the desired vector computation. This applies to the PFL3 computation of the fly's steering signal as well. In that case, the end result is a sinusoidal turning curve given by a scalar cross product (the 2D analog of the 3D vector cross product): for the goal vector $[\cos\theta_g,\ \sin\theta_g]$, where $\theta_g$ is the goal angle, and a heading vector $[\cos\theta_h,\ \sin\theta_h]$, this is $\cos\theta_h\sin\theta_g - \sin\theta_b\cos\theta_g = \sin(\theta_g - \theta_h)$. Any quadratic combination of compass and goal signals that obeys the symmetries imposed by the four-axis coordinate system of the central complex can, at most, give either angle-independent terms, a dot product, or a scalar cross product. In the case of the PFL3s, it gives all three, but the difference between the left and right sides that is the final step of the turning signal computation isolates the scalar cross-product term.

## DISCLOSURE STATEMENT

The authors are not aware of any affiliations, memberships, funding, or financial holdings that might be perceived as affecting the objectivity of this review.

## ACKNOWLEDGMENTS

We thank Richard Axel and Jeremy Dittman for reading the manuscript as well as Max Hoffmann, Sachin Sethi, Sofia Avritzer, Stephen Thornquist, and many other colleagues at The Rockefeller University and Columbia University for useful discussions. This work was supported by a grant from the National Institute of Neurological Disorders and Stroke (R35NS132252) to G.M. L.F.A.

was supported by The Gatsby Charitable Foundation, The Kavli Foundation, and the Simons Collaboration on the Global Brain. G.M. is a Howard Hughes Medical Institute Investigator.

## LITERATURE CITED

Amari S. 1977. Dynamics of pattern formation in lateral-inhibition type neural fields. *Biol. Cybern.* 27:77–87

Arianrhod R. 2024. *Vector: A Surprising Story of Space, Time, and Mathematical Transformation*. University of Chicago Press

Artiushin G, Sehgal A. 2017. The *Drosophila* circuitry of sleep-wake regulation. *Curr. Opin. Neurobiol.* 44:243–50

Basnak MA, Kutschireiter A, Okubo TS, Chen A, Gorelik P, et al. 2025. Multimodal cue integration and learning in a neural representation of head direction. *Nat. Neurosci.* 28:1729–40

Basu J, Nagel K. 2024. Neural circuits for goal-directed navigation across species. *Trends Neurosci.* 47:904–17

Beetz MJ, Kraus C, el Jundi B. 2023. Neural representation of goal direction in the monarch butterfly brain. *Nat. Commun.* 14:5859

Behbahani AH, Palmer EH, Corfas RA, Dickinson MH. 2021. *Drosophila* re-zero their path integrator at the center of a fictive food patch. *Curr. Biol.* 31:4534–46.e5

Ben-Yishai R, Bar-Or RL, Sompolinsky H. 1995. Theory of orientation tuning in visual cortex. *PNAS* 92:3844–48

Braun J, Hurtak F, Wang-Chen S, Ramdya P. 2024. Descending networks transform command signals into population motor control. *Nature* 630:686–94

Chen T-W, Wardill TJ, Sun Y, Pulver SR, Renninger SL, et al. 2013. Ultrasensitive fluorescent proteins for imaging neuronal activity. *Nature* 499:295–300

Collett T, Graham P, Heinze S. 2025. The neuroethology of ant navigation. *Curr. Biol.* 35:R110–24

Corfas RA, Sharma T, Dickinson MH. 2019. Diverse food-sensing neurons trigger idiothetic local search in *Drosophila*. *Curr. Biol.* 29:1660–68.e4

Coyne JA, Boussy IA, Prout T, Bryant SH, Jones JS, Moore JA. 1982. Long-distance migration of *Drosophila*. *Am. Nat.* 119:589–95

Currier TA, Matheson AM, Nagel KI. 2020. Encoding and control of orientation to airflow by a set of *Drosophila* fan-shaped body neurons. *eLife* 9:e61510

Dan C, Hulse BK, Kappagantula R, Jayaraman V, Hermundstad AM. 2024. A neural circuit architecture for rapid learning in goal-directed navigation. *Neuron* 112:2581–99.e23

Dana H, Mohar B, Sun Y, Narayan S, Gordus A, et al. 2016. Sensitive red protein calcium indicators for imaging neural activity. *eLife* 5:e12727

Dana H, Sun Y, Mohar B, Hulse BK, Kerlin AM, et al. 2019. High-performance calcium sensors for imaging activity in neuronal populations and microcompartments. *Nat. Methods* 16:649–57

D'Atri I, DasGupta S. 2025. Neural basis of odometry in *Drosophila*. Preprint, bioRxiv. **https://www.biorxiv.org/content/10.1101/2025.03.23.644782v1**

De J, Wu M, Lambatan V, Hua Y, Joiner WJ. 2023. Re-examining the role of the dorsal fan-shaped body in promoting sleep in *Drosophila*. *Curr. Biol.* 33:3660–68.e4

Donlea JM, Thimgan MS, Suzuki Y, Gottschalk L, Shaw PJ. 2011. Inducing sleep by remote control facilitates memory consolidation in *Drosophila*. *Science* 332:1571–76

Dorkenwald S, Matsliah A, Sterling AR, Schlegel P, Yu S, et al. 2024. Neuronal wiring diagram of an adult brain. *Nature* 634:124–38

Eckstein N, Bates AS, Champion A, Du M, Yin Y, et al. 2024. Neurotransmitter classification from electron microscopy images at synaptic sites in *Drosophila melanogaster*. *Cell* 187:2574–94.e23

Egelhaaf M. 2023. Optic flow based spatial vision in insects. *J. Comp. Physiol. A* 209:541–61

el Jundi B, Foster JJ, Khaldy L, Byrne MJ, Dacke M, Baird E. 2016. A snapshot-based mechanism for celestial orientation. *Curr. Biol.* 26:1456–62

Feng K, Khan M, Minegishi R, Müller A, Van De Poll MN, et al. 2024. A central steering circuit in *Drosophila*. Preprint, bioRxiv. **https://www.biorxiv.org/content/10.1101/2024.06.27.601106v1**

Fisher YE. 2022. Flexible navigational computations in the *Drosophila* central complex. *Curr. Opin. Neurobiol.* 73:102514

Fisher YE, Lu J, D'Alessandro I, Wilson RI. 2019. Sensorimotor experience remaps visual input to a heading-direction network. *Nature* 576:121–25

Fisher YE, Marquis M, D'Alessandro I, Wilson RI. 2022. Dopamine promotes head direction plasticity during orienting movements. *Nature* 612:316–322

Flores-Valle A, Honnef R, Seelig JD. 2022. Automated long-term two-photon imaging in head-fixed walking *Drosophila*. *J. Neurosci. Methods* 368:109432

Garner D, Kind E, Lai JYH, Nern A, Zhao A, et al. 2024. Connectomic reconstruction predicts visual features used for navigation. *Nature* 634:181–90

Giraldo YM, Leitch KJ, Ros IG, Warren TL, Weir PT, Dickinson MH. 2018. Sun navigation requires compass neurons in *Drosophila*. *Curr. Biol.* 28:2845–52.e4

Gohl DM, Silies MA, Gao XJ, Bhalerao S, Luongo FJ, et al. 2011. A versatile in vivo system for directed dissection of gene expression patterns. *Nat. Methods* 8:231–37

Goulard R, Heinze S, Webb B. 2023. Emergent spatial goals in an integrative model of the insect central complex. *PLOS Comput. Biol.* 19:e1011480

Govorunova EG, Sineshchekov OA, Janz R, Liu X, Spudich JL. 2015. Natural light-gated anion channels: a family of microbial rhodopsins for advanced optogenetics. *Science* 349:647–50

Green J, Adachi A, Shah KK, Hirokawa JD, Magani PS, Maimon G. 2017. A neural circuit architecture for angular integration in *Drosophila*. *Nature* 546:101–6

Green J, Maimon G. 2018. Building a heading signal from anatomically defined neuron types in the *Drosophila* central complex. *Curr. Opin. Neurobiol.* 52:156–64

Green J, Vijayan V, Mussells Pires P, Adachi A, Maimon G. 2019. A neural heading estimate is compared with an internal goal to guide oriented navigation. *Nat. Neurosci.* 22:1460–68

Hanesch U, Fischbach K, Heisenberg M. 1989. Neuronal architecture of the central complex in *Drosophila melanogaster*. *Cell Tissue Res.* 257:343–66

Hardcastle BJ, Omoto JJ, Kandimalla P, Nguyen B-CM, Keleş MF, et al. 2021. A visual pathway for skylight polarization processing in *Drosophila*. *eLife* 10:e63225

Hartmann G, Wehner R. 1995. The ant's path integration system: a neural architecture. *Biol. Cybern.* 73:483–97

Hasenhuetl PS, Sarnataro R, Vrontou E, Rorsman HO, Talbot CB, Brain R, Miesenboeck G. 2024. A half-centre oscillator encodes sleep pressure. Preprint, bioRxiv. **https://www.biorxiv.org/content/10.1101/2024.02.23.581780v1**

Heinze S. 2024. Variations on an ancient theme—the central complex across insects. *Curr. Opin. Behav. Sci.* 57:101390

Heinze S, Homberg U. 2007. Maplike representation of celestial E-vector orientations in the brain of an insect. *Science* 315:995–97

Heinze S, Homberg U. 2008. Neuroarchitecture of the central complex of the desert locust: intrinsic and columnar neurons. *J. Comp. Neurol.* 511:454–78

Heinze S, Narendra A, Cheung A. 2018. Principles of insect path integration. *Curr. Biol.* 28:R1043–58

Heisenberg M, Wolf R. 1984. *Vision in* Drosophila*: Genetics of Microbehavior*. Springer-Verlag

Henning M, Ramos-Traslosheros G, Gür B, Silies M. 2022. Populations of local direction-selective cells encode global motion patterns generated by self-motion. *Sci. Adv.* 8:eabi7112

Honkanen A, Adden A, da Silva Freitas J, Heinze S. 2019. The insect central complex and the neural basis of navigational strategies. *J. Exp. Biol.* 222:jeb188854

Huang C, Maxey JR, Sinha S, Savall J, Gong Y, Schnitzer MJ. 2018. Long-term optical brain imaging in live adult fruit flies. *Nat. Commun.* 9:872

Hulse BK, Haberkern H, Franconville R, Turner-Evans D, Takemura S, et al. 2021. A connectome of the *Drosophila* central complex reveals network motifs suitable for flexible navigation and context-dependent action selection. *eLife* 10:e66039

Hulse BK, Jayaraman V. 2020. Mechanisms underlying the neural computation of head direction. *Annu. Rev. Neurosci.* 43:31–54

Hulse BK, Stanoev A, Turner-Evans DB, Seelig JD, Jayaraman V. 2023. A rotational velocity estimate constructed through visuomotor competition updates the fly's neural compass. Preprint, bioRxiv. **https://www.biorxiv.org/content/10.1101/2023.09.25.559373v1**

Ishida IG, Sethi S, Mohren TL, Haraguchi M, Abbott LF, Maimon G. 2025. Neuronal calcium spikes enable vector inversion in the *Drosophila* brain. *Cell* 189:748–64

Iwano M, Hill ES, Mori A, Mishima T, Mishima T, et al. 2010. Neurons associated with the flip-flop activity in the lateral accessory lobe and ventral protocerebrum of the silkworm moth brain. *J. Comp. Neurol.* 518:366–88

Jenett A, Rubin GM, Ngo T-TB, Shepherd D, Murphy C, et al. 2012. A GAL4-driver line resource for *Drosophila* neurobiology. *Cell Rep*. 2:991–1001

Kathman ND, Lanz AJ, Freed JD, Nagel KI. 2024. Neural dynamics for working memory and evidence integration during olfactory navigation in *Drosophila*. Preprint, bioRxiv. **https://www.biorxiv.org/content/10.1101/2024.10.05.616803v1**

Kempf A, Song SM, Talbot CB, Miesenböck G. 2019. A potassium channel β-subunit couples mitochondrial electron transport to sleep. *Nature* 568:230–34

Kim IS, Dickinson MH. 2017. Idiothetic path integration in the fruit fly *Drosophila melanogaster*. *Curr. Biol.* 27:2227–38.e3

Kim SS, Hermundstad AM, Romani S, Abbott LF, Jayaraman V. 2019. Generation of stable heading representations in diverse visual scenes. *Nature* 576:126–31

Kim SS, Rouault H, Druckmann S, Jayaraman V. 2017. Ring attractor dynamics in the *Drosophila* central brain. *Science* 356:849–53

Klapoetke NC, Murata Y, Kim SS, Pulver SR, Birdsey-Benson A, et al. 2014. Independent optical excitation of distinct neural populations. *Nat. Methods* 11:338–46

Krapp HG. 2000. Neuronal matched filters for optic flow processing in flying insects. In *International Review of Neurobiology: Neuronal Processing of Optic Flow*, ed. M Lappe. Academic Press

Kvon EZ, Kazmar T, Stampfel G, Yáñez-Cuna JO, Pagani M, et al. 2014. Genome-scale functional characterization of *Drosophila* developmental enhancers in vivo. *Nature* 512:91–95

Le Moël F, Stone T, Lihoreau M, Wystrach A, Webb B. 2019. The central complex as a potential substrate for vector based navigation. *Front. Psychol.* 10:690

Leitch KJ, Ponce FV, Dickson WB, van Breugel F, Dickinson MH. 2021. The long-distance flight behavior of *Drosophila* supports an agent-based model for wind-assisted dispersal in insects. *PNAS* 118:e2013342118

Lima SQ, Miesenböck G. 2005. Remote control of behavior through genetically targeted photostimulation of neurons. *Cell* 121:141–52

Lin C-Y, Chuang C-C, Hua T-E, Chen C-C, Dickson BJ, et al. 2013. A comprehensive wiring diagram of the protocerebral bridge for visual information processing in the *Drosophila* brain. *Cell Rep*. 3:1739–53

Liu S, Liu Q, Tabuchi M, Wu MN. 2016. Sleep drive is encoded by neural plastic changes in a dedicated circuit. *Cell* 165:1347–60

Liu W, Liu C, Ren P-G, Chu J, Wang L. 2022. An improved genetically encoded fluorescent cAMP indicator for sensitive cAMP imaging and fast drug screening. *Front. Pharmacol.* 13:902290

Lu J, Behbahani AH, Hamburg L, Westeinde EA, Dawson PM, et al. 2021. Transforming representations of movement from body- to world-centric space. *Nature* 601:98–104

Lyu C, Abbott LF, Maimon G. 2021. Building an allocentric travelling direction signal via vector computation. *Nature* 601:92–97

Maimon G, Straw AD, Dickinson MH. 2010. Active flight increases the gain of visual motion processing in *Drosophila*. *Nat. Neurosci.* 13:393–99

Marr D. 1982. *Vision: A Computational Investigation into the Human Representation and Processing of Visual Information*. Henry Holt and Co.

Matheson AMM, Lanz AJ, Medina AM, Licata AM, Currier TA, et al. 2022. A neural circuit for wind-guided olfactory navigation. *Nat. Commun.* 13:4613

Mauss AS, Borst A. 2020. Optic flow-based course control in insects. *Curr. Opin. Neurobiol.* 60:21–27

May C, Cellini B, Van Breugel F, Nagel K. 2025. A compact multisensory representation of self-motion is sufficient for computing an external world variable. Preprint, bioRxiv. **https://www.biorxiv.org/content/10.1101/2025.05.09.653128v1.full**

Meissner GW, Vannan A, Jeter J, Close K, DePasquale GM, et al. 2025. A split-GAL4 driver line resource for *Drosophila* neuron types. Preprint, *eLife* 13:RP98405. **https://elifesciences.org/articles/98405**

Mitchell R, Shaverdian S, Dacke M, Webb B. 2023. A model of cue integration as vector summation in the insect brain. *Proc. R. Soc. B* 290:20230767

Mohammad F, Stewart JC, Ott S, Chlebikova K, Chua JY, et al. 2017. Optogenetic inhibition of behavior with anion channelrhodopsins. *Nat. Methods* 14:271–74

Mussells Pires P, Zhang L, Parache V, Abbott LF, Maimon G. 2024. Converting an allocentric goal into an egocentric steering signal. *Nature* 626:808–18

Namiki S, Ros IG, Morrow C, Rowell WJ, Card GM, Korff W, Dickinson MH. 2022. A population of descending neurons that regulates the flight motor of *Drosophila*. *Curr. Biol.* 32:1189–96.e6

Nern A, Pfeiffer BD, Rubin GM. 2015. Optimized tools for multicolor stochastic labeling reveal diverse stereotyped cell arrangements in the fly visual system. *PNAS* 112:E2967–76

Noorman M, Hulse BK, Jayaraman V, Romani S, Hermundstad AM. 2024. Maintaining and updating accurate internal representations of continuous variables with a handful of neurons. *Nat. Neurosci.* 27:2207–17

O'Keefe J. 1991. An allocentric spatial model for the hippocampal cognitive map. *Hippocampus* 1:230–35

Okubo TS, Patella P, D'Alessandro I, Wilson RI. 2020. A neural network for wind-guided compass navigation. *Neuron* 107:924–40.e18

Omoto JJ, Keleş MF, Nguyen B-CM, Bolanos C, Lovick JK, et al. 2017. Visual input to the *Drosophila* central complex by developmentally and functionally distinct neuronal populations. *Curr. Biol.* 27:1098–110

Petrucco L, Lavian H, Wu YK, Svara F, Štih V, Portugues R. 2023. Neural dynamics and architecture of the heading direction circuit in zebrafish. *Nat. Neurosci.* 26:765–73

Pfeiffer K, Homberg U. 2014. Organization and functional roles of the central complex in the insect brain. *Annu. Rev. Entomol.* 59:165–84

Pimentel D, Donlea JM, Talbot CB, Song SM, Thurston AJF, Miesenböck G. 2016. Operation of a homeostatic sleep switch. *Nature* 536:333–37

Pisokas I, Rössler W, Webb B, Zeil J, Narendra A. 2022. Anesthesia disrupts distance, but not direction, of path integration memory. *Curr. Biol.* 32:445–52.e4

Plitt MH, Turner-Evans DB, Co JC, Layden A, Eddison M, et al. 2025. Octopamine instructs head direction plasticity. Preprint, bioRxiv. **https://www.biorxiv.org/content/10.64898/2025.12.11.693783v1**

Poggio T. 2012. The levels of understanding framework, revised. *Perception* 41:1017–23

Rayshubskiy A, Holtz SL, Bates AS, Vanderbeck QX, Serratosa Capdevila L, Rockwell V, Wilson R. 2025. Neural circuit mechanisms for steering control in walking *Drosophila*. Preprint, *eLife* 13:RP102230. **https://elifesciences.org/articles/102230**

Redish AD, Elga AN, Touretzky DS. 1996. A coupled attractor model of the rodent head direction system. *Netw. Comput. Neural Syst.* 7:671–85

Rorsman HO, Müller MA, Liu PZ, Sanchez LG, Kempf A, et al. 2025. Sleep pressure accumulates in a voltage-gated lipid peroxidation memory. *Nature* 641:232–39

Sarnataro R, Velasco CD, Monaco N, Kempf A, Miesenböck G. 2025. Mitochondrial origins of the pressure to sleep. *Nature* 645:722–28

Scheffer LK, Xu CS, Januszewski M, Lu Z, Takemura S, et al. 2020. A connectome and analysis of the adult *Drosophila* central brain. *eLife* 9:e57443

Schlegel P, Yin Y, Bates AS, Dorkenwald S, Eichler K, et al. 2023. A consensus cell type atlas from multiple connectomes reveals principles of circuit stereotypy and variation. Preprint, bioRxiv. **https://www.biorxiv.org/content/10.1101/2023.06.27.546055v1**

Schnell B, Ros IG, Dickinson MH. 2017. A descending neuron correlated with the rapid steering maneuvers of flying *Drosophila*. *Curr. Biol.* 27:1200–5

Seelig J, Chiappe M, Lott G, Dutta A, Osborne J, Reiser M, Jayaraman V. 2010. Two-photon calcium imaging from head-fixed *Drosophila* during optomotor walking behavior. *Nat. Methods* 7:535–40

Seelig JD, Jayaraman V. 2013. Feature detection and orientation tuning in the *Drosophila* central complex. *Nature* 503:262–66

Seelig JD, Jayaraman V. 2015. Neural dynamics for landmark orientation and angular path integration. *Nature* 521:186–91

Sharp PE, Blair HT, Brown M. 1996. Neural network modeling of the hippocampal formation spatial signals and their possible role in navigation: a modular approach. *Hippocampus* 6:720–34

Siliciano A, Sun M, Morton C, Dowell C, Eghbali N, et al. 2025. A vector-based strategy for olfactory navigation in *Drosophila*. Preprint, bioRxiv. **https://www.biorxiv.org/content/10.1101/2025.02.15.638426v1**

Skaggs WE, Knierim JJ, Kudrimoti HS, McNaughton BL. 1995. A model of the neural basis of the rat's sense of direction. *Adv. Neural Inf. Process. Syst.* 7:173–80

Stone T, Webb B, Adden A, Weddig NB, Honkanen A, et al. 2017. An anatomically constrained model for path integration in the bee brain. *Curr. Biol.* 27:3069–85.e11

Strausfeld NJ. 2012. *Arthropod Brains: Evolution, Functional Elegance, and Historical Significance*. Harvard University Press

Stupski SD, Van Breugel F. 2024. Wind gates olfaction-driven search states in free flight. *Curr. Biol.* 34:4397–411.e6

Tirian L, Dickson BJ. 2017. The VT GAL4, LexA, and split-GAL4 driver line collections for targeted expression in the *Drosophila* nervous system. Preprint, bioRxiv. **https://www.biorxiv.org/content/10.1101/198648v1**

Titova AV, Kau BE, Tibor S, Mach J, Vo-Doan TT, et al. 2023. Displacement experiments provide evidence for path integration in *Drosophila*. *J. Exp. Biol.* 226:jeb245289

Touretzky DS, Redish AD, Wan HS. 1993. Neural representation of space using sinusoidal arrays. *Neural Comput.* 5:869–84

Turner-Evans D, Jensen KT, Ali S, Paterson T, Sheridan A, et al. 2020. The neuroanatomical ultrastructure and function of a biological ring attractor. *Neuron* 108:145–63.e10

Turner-Evans D, Wegener S, Rouault H, Franconville R, Wolff T, et al. 2017. Angular velocity integration in a fly heading circuit. *eLife* 6:e04577

Van Breugel F, Jewell R, Houle J. 2022. Active anemosensing hypothesis: how flying insects could estimate ambient wind direction through sensory integration and active movement. *J. R. Soc. Interface* 19:20220258

Vickerstaff RJ, Cheung A. 2010. Which coordinate system for modelling path integration? *J. Theor. Biol.* 263:242–61

von Frisch K. 1967. *The Dance Language and Orientation of Bees*. Harvard University Press

Wang L, Wu C, Peng W, Zhou Z, Zeng J, et al. 2022. A high-performance genetically encoded fluorescent indicator for in vivo cAMP imaging. *Nat. Commun.* 13:5363

Wehner R. 2020. *Desert Navigator: The Journey of an Ant*. Harvard University Press

Weisman JL, Mohren TL, Ryu JD, Wyse MZ, Dias-Ferreira E, Maimon G. 2025. *Drosophila* maintain a consistent navigational goal angle for days to weeks. Preprint, bioRxiv. **https://www.biorxiv.org/content/10.64898/2025.12.09.693277v1**

Westeinde EA, Kellogg E, Dawson PM, Lu J, Hamburg L, et al. 2024. Transforming a head direction signal into a goal-oriented steering command. *Nature* 626:819–26

Williams J. 1975. Anatomical studies of the insect central nervous system: a ground-plan of the midbrain and an introduction to the central complex in the locust, *Schistocerca gregaria* (Orthoptera). *J. Zool.* 176:67–86

Wilson RI. 2023. Neural networks for navigation: from connections to computations. *Annu. Rev. Neurosci.* 46:403–23

Wittmann T, Schwegler H. 1995. Path integration—a network model. *Biol. Cybern.* 73:569–75

Wolf R, Heisenberg M. 1991. Basic organization of operant behavior as revealed in *Drosophila* flight orientation. *J. Comp. Physiol.* 169:699–705

Wolff T, Eddison M, Chen N, Nern A, Sundaramurthi P, et al. 2025. Cell type-specific driver lines targeting the *Drosophila* central complex and their use to investigate neuropeptide expression and sleep regulation. Preprint, *eLife* 14:RP104764. **https://elifesciences.org/articles/104764**

Wolff T, Iyer NA, Rubin GM. 2015. Neuroarchitecture and neuroanatomy of the *Drosophila* central complex: a GAL4-based dissection of protocerebral bridge neurons and circuits. *J. Comp. Neurol.* 523:997–1037

Wolff T, Rubin GM. 2018. Neuroarchitecture of the *Drosophila* central complex: a catalog of nodulus and asymmetrical body neurons and a revision of the protocerebral bridge catalog. *J. Comp. Neurol.* 526:2585–611

Yang HH, Brezovec BE, Serratosa Capdevila L, Vanderbeck QX, Adachi A, et al. 2024. Fine-grained descending control of steering in walking *Drosophila*. *Cell* 187:6290–308.e27

Young JM, Armstrong JD. 2010a. Structure of the adult central complex in *Drosophila*: organization of distinct neuronal subsets. *J. Comp. Neurol.* 518:1500–24

Young JM, Armstrong JD. 2010b. Building the central complex in *Drosophila*: the generation and development of distinct neural subsets. *J. Comp. Neurol.* 518:1525–41

Zemelman BV, Lee GA, Ng M, Miesenböck G. 2002. Selective photostimulation of genetically chARGed neurons. *Neuron* 33:15–22

Zhang K. 1996. Representation of spatial orientation by the intrinsic dynamics of the head-direction cell ensemble: a theory. *J. Neurosci.* 16:2112–26

Zhao A, Gruntman E, Nern A, Iyer NA, Rogers EM, et al. 2025. Eye structure shapes neuron function in *Drosophila* motion vision. *Nature* 646:135–42

Zheng Z, Lauritzen JS, Perlman E, Robinson CG, Nichols M, et al. 2018. A complete electron microscopy volume of the brain of adult *Drosophila melanogaster*. *Cell* 174:730–43.e22

Ziegler PE, Wehner R. 1997. Time-courses of memory decay in vector-based and landmark-based systems of navigation in desert ants, *Cataglyphis fortis*. *J. Comp. Physiol. A* 181:13–20